



# Journal of Applied Sciences

ISSN 1812-5654

**science**  
alert

**ANSI***net*  
an open access publisher  
<http://ansinet.com>

## Performance of the Push-Pull LLC Resonant and PWM ZVS Full Bridge Topologies

Deepak Kumar Nayak and S. Rama Reddy

Department of Electrical and Electronics Engg, Jerusalem College of Engg,  
Centre for Collaborative Research with Anna University, Palikaranai, Chennai-601302, India

---

**Abstract:** The soft switched PWM ZVS full bridge DC to DC converter and push-pull type LLC series resonant converter are compared for use in low output voltage power supply applications. It is shown that push-pull type LLC series resonant converter takes on the desirable characteristics of the conventional push-pull converter and LLC series resonant converter. Push-pull type has less conduction loss than that of full bridge converter. Analyses and simulation shows that for low power applications required turn ratio of the transformer is less so efficiency is more and switching stress is less for push-pull LLC series resonant converter than PWM ZVS full bridge DC to DC converter. The 48V DC is efficiently reduced to 12V DC using both DC to DC converters using 20KHZ switching frequency and all parameters are compared.

**Key words:** DC-DC converter, full bridge converter, soft-switching, phase shift (PS), zero voltage switching (ZVS)

---

### INTRODUCTION

Now-a-days the kinds of control type soft switching circuits are few. Phase shifted full-bridge converter, asymmetrical half-bridge converter push-pull converter and LLC series resonant converters and so on are the typical topologies.

The Full-Bridge (FB) Zero-Voltage-Switched (ZVS) converter is one of the most attractive techniques. It is the most widely used soft-switched circuit in high-power applications (Redl *et al.*, 1991; Sabate *et al.*, 1991; Chen *et al.*, 1995). This constant-frequency converter employs Phase-Shift (PS) control and features ZVS of the primary switches with relatively small circulating energy. In this technique a control circuit serves to supply pulsed control signals to the switching transistors of the converter for maintaining the output voltage at its desired level using phase shift control in known manner. Though the snubber approaches in (Redl *et al.*, 1991; Sabate *et al.*, 1991) offer practical and efficient solutions to the secondary-side ringing problem, they do not offer any improvement of the secondary-side duty-cycle loss.

Several techniques have been proposed to extend the ZVS range of FB ZVS converters without the loss of duty cycle and secondary-side ringing (Jain *et al.*, 2002; Ayyanar and Mohan, 2001; Mason and Jain, 2005; Jang and Jovanovic, 2004). Generally these circuits utilize energy stored in the inductive components of an auxiliary circuit to achieve ZVS for all primary switches in an

extended load and input voltage range. Ideally, the auxiliary circuit needs to provide very little energy, if any, at full load because the full-load current stores enough energy in the converter's inductive components to achieve complete ZVS for all switches. As the load current decreases the energy provided by the auxiliary circuit must increase to maintain ZVS with the maximum energy required at no load. The energy stored for ZVS is independent of load as described by Jain *et al.* (2002) and Ayyanar and Mohan, (2001). Adaptive energy storage in the auxiliary circuit has been given by Mason and Jain (2005) and Jang and Jovanovic (2004). However, these converters have to use large inductors so; high circulating energy is needed to achieve no-load ZVS. ZVS full bridge DC to DC converter with ZVS over the entire range is given by Borage *et al.* (2008). High power density multikilowatt DC to DC converter with galvanic isolation is given by Pavlovsky *et al.* (2009).

Conventional push-pull converter is used in low and medium power systems for the reason of less conduction loss than that of half bridge or full bridge converters and low side driving of both primary switches. As featuring in ZVS for primary switches over entire load ZCS for rectifier diodes wide input voltage range capability and high efficiency under all input voltages the LLC series resonant converter gains popularity in recent years (Lee *et al.*, 2002; Wei *et al.*, 2007).

Push-pull type LLC-SRC combines characteristics of both conventional push-pull converter and LLC series

resonant converter. An LCL resonant push-pull topology operating under ZVS condition was presented by Ryan *et al.* (1998). The circuit exhibits ZVS for the MOSFET switches and the resonant capacitor snubs the reverse recovery transient of rectifier diodes. Since the load of this topology is series connected with the resonant inductor the output current will swing corresponding to the resonant current and it's difficult to reduce the ripple of output voltage. An LC resonant push-pull topology was presented in which the primary switches and secondary rectifiers turn on and turn off under zero-voltage and zero-current switching conditions respectively Boonyaroonate and Mori (2002). With most of the resonant current flowing through the output capacitor it's easy to control the ripple of output voltage. But for resonant converters the large current or voltage stress on switching elements and higher conduction loss are difficult to control. Detail stage equations for each stage and design process for a conventional LLC series resonant converter have been proposed by Liu *et al.* (2006). High dc gain step-up push-pull type LLC series resonant DC-DC converter is proposed by Chen *et al.* (2008). The analysis of series-parallel resonant DC-to-DC converter has been illustrated by Padmanabhan *et al.* (2007). The above literature does not deal with comparison of push-pull LLC and PWM ZVS FB converters.

In this study, a FB ZVS converter with adaptive energy storage that offers ZVS of the primary switches over a wide load range with greatly reduced no-load circulating energy and with significantly reduced secondary-side duty cycle loss is considered for comparison with push-pull LLC series resonant converter.

### OPERATIONAL PRINCIPLE OF FB ZVS CONVERTER

The circuit diagram of the FB ZVS converter is shown in Fig. 1. In the circuit since the ZVS energy stored in the primary inductor is dependent on its inductance value and the volt-second product of the secondary of auxiliary transformer TRA the size of the primary inductor can be minimized by properly selecting the turn ratio of auxiliary transformer TRA. As a result the size of the primary inductor is very much reduced compared to that of the conventional PS FB converter. In addition since the auxiliary transformer does not need to store energy, its size can be small. Finally because the energy used to create the ZVS condition at light loads is not stored in the leakage inductances of transformer Tr the transformer's leakage inductances can also be minimized. As a result of the reduced total primary inductance i.e. the inductance of the primary inductor used for ZVS energy storage and the leakage inductance of the power transformer the modified converter exhibits a relatively small duty-cycle loss. This minimizes both the conduction loss of the primary switches and the voltage stress on the components on the secondary side of the transformer which improves the conversion efficiency. Moreover, because of the reduced total primary inductance the secondary side parasitic ringing is also reduced and is effectively controlled by primary side diodes D and D<sub>1</sub> as shown in Fig. 1.

**Technical specifications of Fig. 1:** DC input voltage = 48V,  $V_p = 0.01 \mu H$ ,  $R = 25\Omega$ ,  $L_1 = 28\mu H$ ,  $C_7 = 120\mu F$ ,  $C_5 = 0.5\mu F$ ,  $C_6 = 12\mu F$ , Operating frequency = 20 KHz.

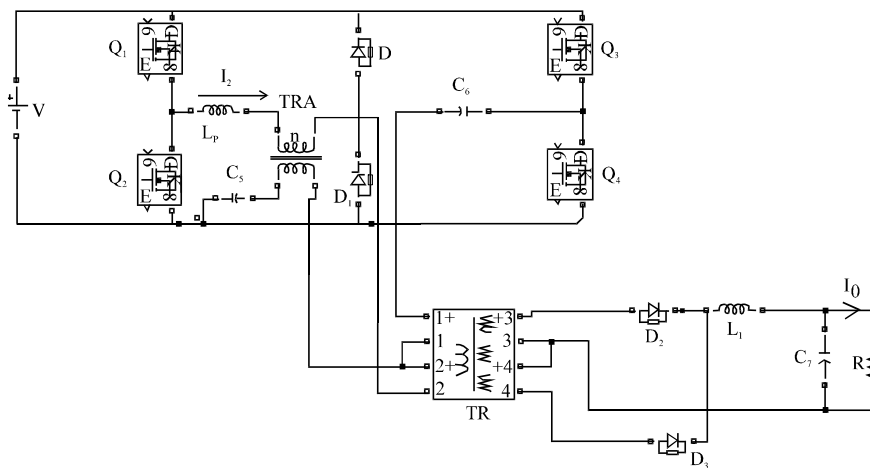


Fig. 1: FB ZVS converter

To achieve ZVS energy stored in the primary inductor  $L_p(E_{LP})$  must be higher than total energy required to charge  $C_1$  and discharge  $C_2$ :

$$E_{LP} \geq CV^2 \tag{1}$$

where,  $C_1 = C_2 = C$ . = Capacitance across  $Q_1$  and  $Q_2$  respectively:

$$E_{LP} = \frac{1}{2} L_P \left[ \frac{I_0}{n} + V \left( \frac{1-T}{4n_1 L_P f_s} \right) \right] \tag{2}$$

where,  $f_s$  is the switching frequency and T is the duty cycle of switch:

- $n$  = Main transformer turn ratio
- $n_1$  = Auxiliary transformer turn ratio.

**OPERATIONAL PRINCIPLE OF PUSH-PULL LLC SERIES RESONANT CONVERTER**

Power stage of the modified push-pull LLC series resonant converter is shown in Fig. 2. The main components of the converter are: two main switches  $Q_1$  and  $Q_2$  constitute the two push-pull branches respectively. The DC to DC converter further includes a resonant tank connected to the secondary of transformer comprising a series capacitor connected to a series inductor and a parallel inductor. The components of resonant tank are  $L_{ss}C_r$  and  $L_{sr}$ .  $C_1$  and  $C_2$  represent parasitic capacitor of  $Q_1$  and  $Q_2$  respectively. The output rectifier consists of four diodes  $D_1$ - $D_4$ .

**Technical specifications of Fig. 2:** DC input voltage = 48V,  $L_{s1} = 0.11 \mu H$ ,  $L_{s2} = 0.13 \mu H$ ,  $C_1 = C_2 = 0.01 * 10^{-11} F$ ,  $L_{ss} = 19.8 \mu H$ ,  $L_{sr} = 6.32 mH$ ,  $C_r = 3.06 \mu F$ ,  $C_0 = 300 \mu F$ ,  $R = 25 \Omega$  Operating frequency = 20 KHz.

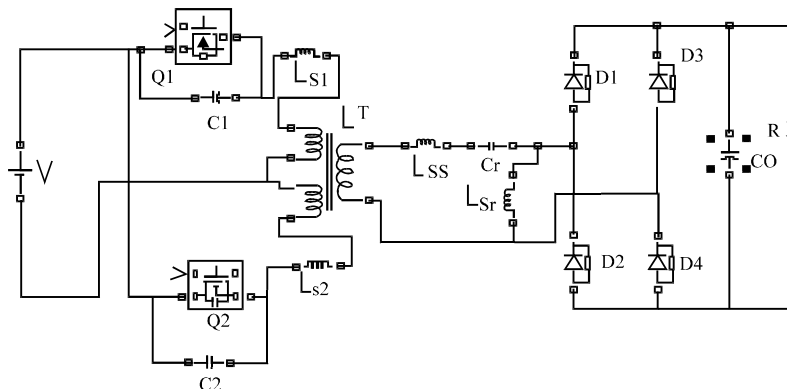


Fig. 2: Push-Pull LLC series resonant converter

The control strategy is similar to a conventional LLC series resonant converter i.e.,  $Q_1$  and  $Q_2$  conduct alternately in a switching cycle under variable frequency modulation. It is assumed that the converter is under steady operation and the output capacitor  $C_0$  is large enough to be considered as a voltage source. The series capacitor functioning with the series inductor provide a first characteristic resonant frequency represented by  $f_s$  and the series capacitor functioning with the series inductor and the parallel inductor to provide a second characteristic resonant frequency represented by  $f_m$  where  $f_s > f_m$ :

$$f_s = \frac{1}{2\pi\sqrt{L_{ss}C_r}} \tag{3}$$

$$f_m = \frac{1}{2\pi\sqrt{(L_{ss} + L_{sr})C_r}} \tag{4}$$

When the operation frequency is between first and second resonant frequency i.e.  $f_m < f < f_s$  the switches operate under zero-voltage-switching condition and the rectifier circuit operate under zero-current-switching condition. Fig. 4 has drawn when  $f_m < f < f_s$

The boundary conditions for ZVS can be obtained according to energy balance:

$$\frac{1}{2} [n^2 (L_{ss} + L_{sr})] \left( \frac{I_{Lsr}}{2n} \right)^2 = \frac{1}{2} 2C_s (2V)^2 \tag{5}$$

where, n is the transformer turns ratio.  $I_{Lsr}$  is the current across  $L_{sr}$

**SIMULATION RESULTS OF FB ZVS CONVERTER**

The ZVS DC to DC converter is simulated using matlab simulink and the results are presented here.

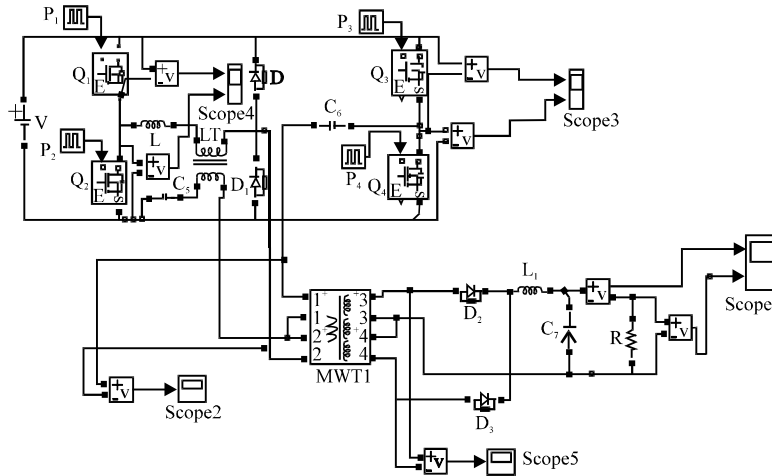


Fig. 3: Simulink model of FB ZVS DC to DC converter

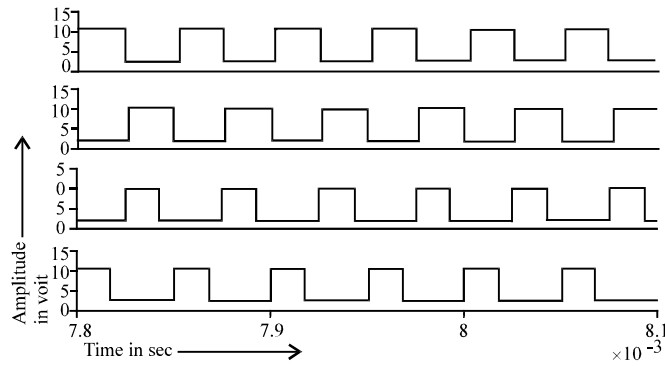


Fig. 4: Driving pulses

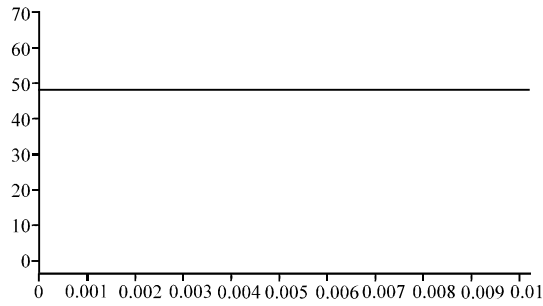


Fig. 5: DC input voltage

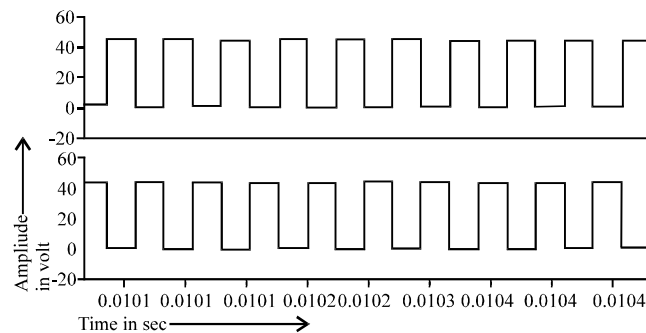


Fig. 6: Output voltage across  $Q_1$  and  $Q_2$

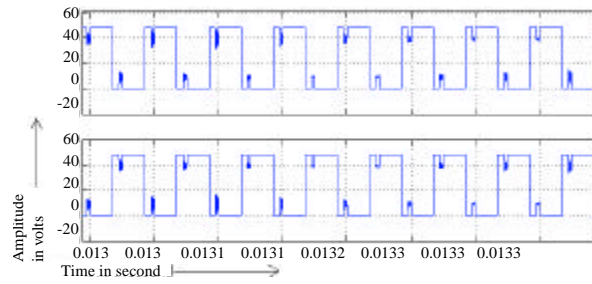


Fig. 7: Output voltage across  $Q_3$  and  $Q_4$

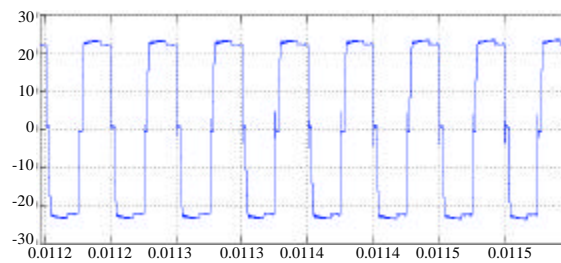


Fig. 8: Voltage across the secondary

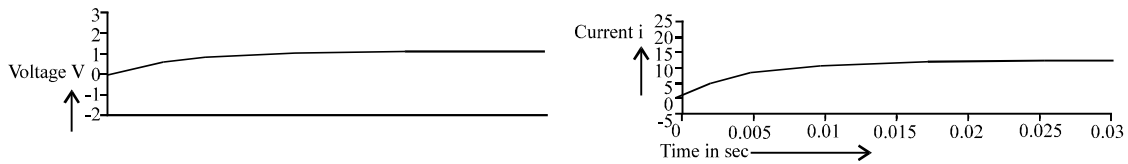


Fig. 9: DC output current and voltage

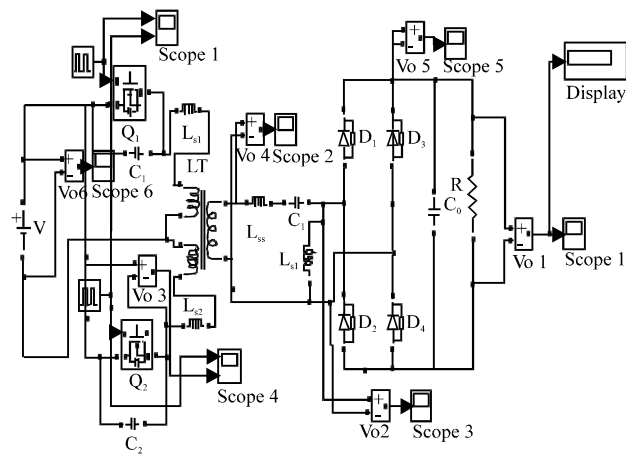


Fig. 10: Simulink model of modified LLC SRC

Simulink model of FB ZVS DC to DC converter is shown in Fig. 3. Driving pulses are shown in Fig. 4. DC input voltage is shown in Fig. 5. Output voltage across  $Q_1$  and  $Q_2$  is shown in Fig. 6. Voltage across  $Q_3$  and  $Q_4$  are shown in Fig. 7. Secondary voltage is shown in Fig. 8. DC output current and voltage are shown in Fig. 9. DC output voltage is 12V and the current 1A. It can be seen that the DC output is free from ripple.

For constant-frequency variable duty cycle control of the proposed converter switches  $Q_1$  and  $Q_2$  always operate with approximately 50% duty cycle whereas switches  $Q_3$  and  $Q_4$  have a duty cycle in the range from 0 to 50% as shown in Fig. 5.

**SIMULATION RESULTS OF PUSH-PULL LLC SERIES RESONANT CONVERTER**

The ZVS push-pull LLC series resonant converter is simulated using matlab simulink and the results are presented here.

Simulink model of LLC series resonant converter is shown in Fig. 10. Driving pulses are shown in Fig. 11. DC input voltage is shown in Fig. 12. Drain to source voltage across switch  $Q_1$  is shown in Fig. 13. Secondary voltage is shown in Fig. 14. Voltage across  $L_{sr}$  is shown in Fig. 15. DC output current and voltage is shown in Fig. 16. DC output voltage is 12V and the current is 2.46A. It can be shown that DC output voltage is free from ripple.

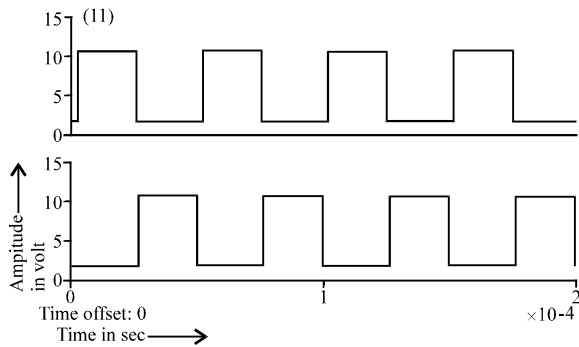


Fig. 11: Driving pulses

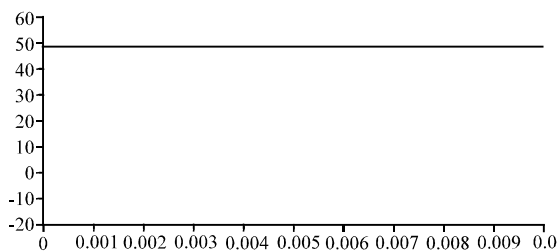


Fig. 12: DC input voltage

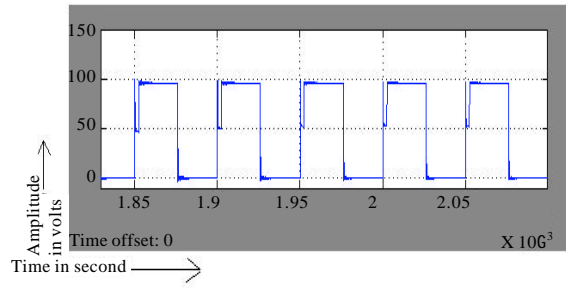


Fig. 13: Drain to source voltage across switch  $Q_1$

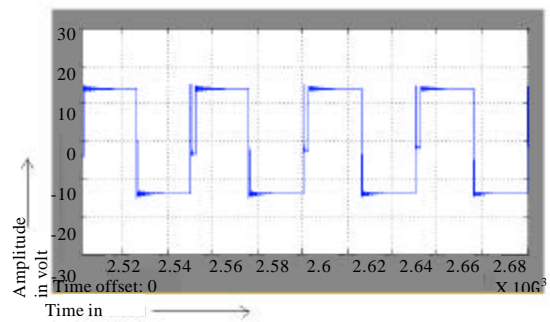


Fig. 14: Secondary voltage of transformer

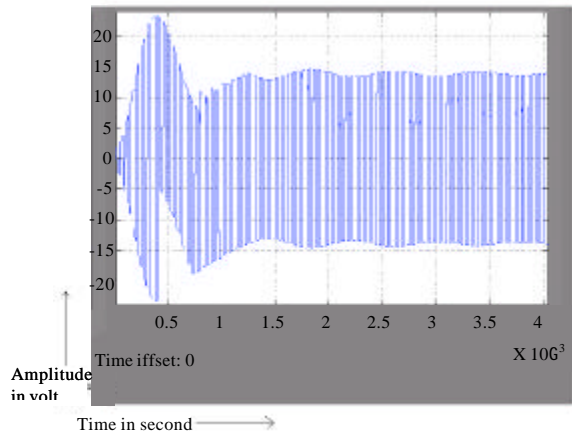


Fig. 15: Voltage across  $L_{sr}$

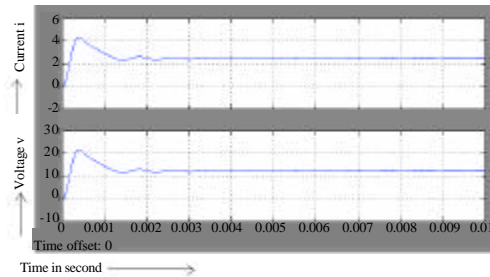


Fig. 16: DC output current and voltage

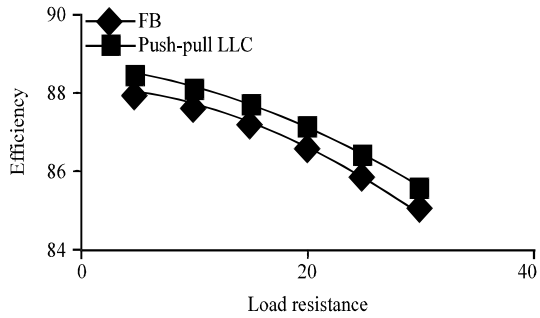


Fig. 17: Efficiency versus load resistance

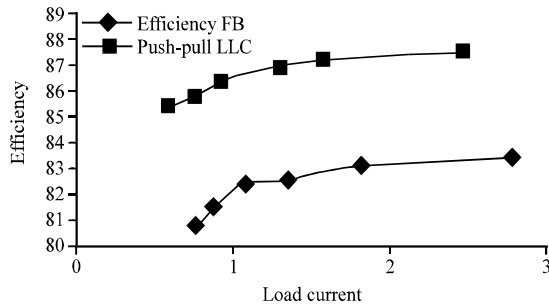


Fig. 18: Load current versus efficiency from simulation

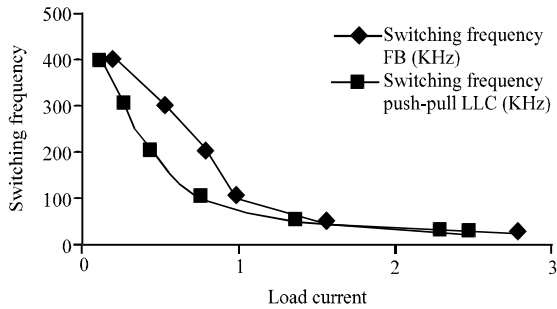


Fig. 19: Load current versus switching frequency from simulation

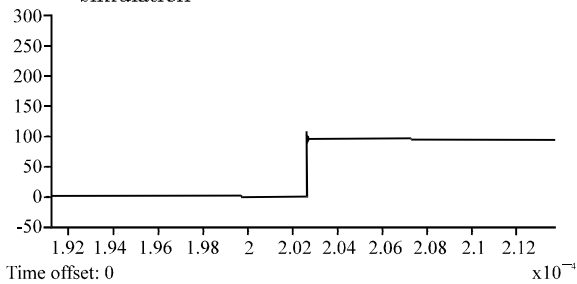


Fig. 20: Switch stress for push-pull LLC

Fig. 17 shows the variation of efficiency with load resistance. Fig. 18 shows load current versus efficiency from simulation. Fig. 19 shows load current versus switching frequency from simulation. Fig. 20 shows switch stress for push-pull LLC converter and Fig. 21 shows switch stress for FB ZVS converter.

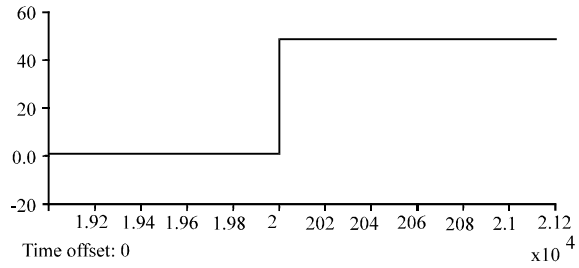


Fig. 21: Switch stress for FB ZVS

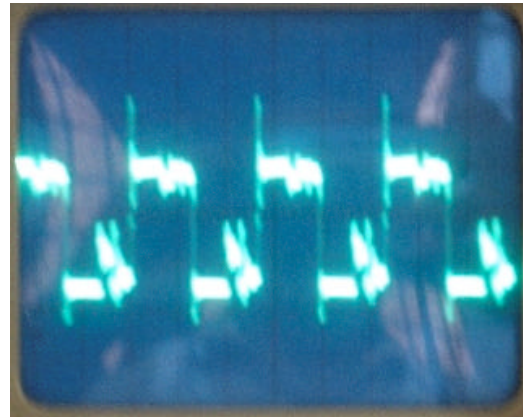


Fig. 22: Voltage across the primary X axis 1 div = 0.02 m sec Y axis 1 div = 20 V

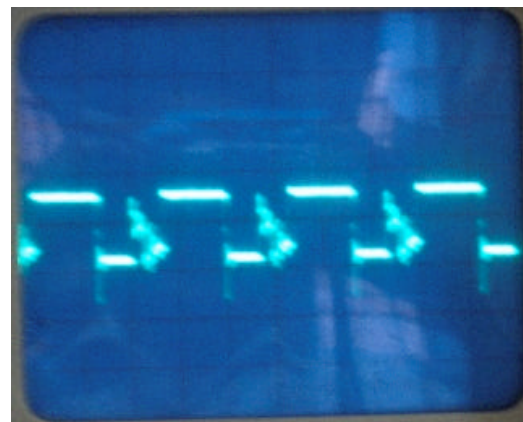


Fig. 23: Voltage across the secondary X axis 1 div = 0.02 m sec, Y axis 1 div = 30 V

### EXPERIMENTAL VERIFICATION OF FB ZVS CONVERTER

The DC to DC converter was built and tested at 48 V DC. The circuit parameters are as follows.



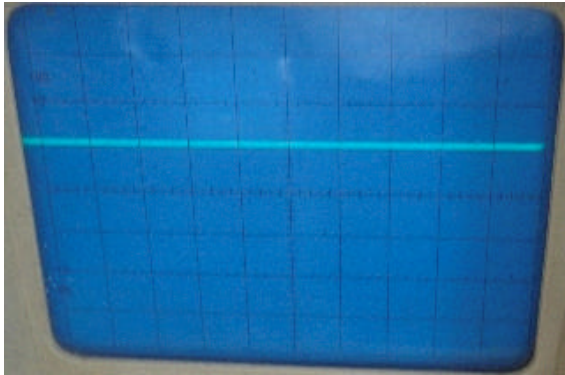


Fig. 24: Oscillogram of load voltage X axis 1 div = 0.02 m sec, Y axis 1 div = 10 V

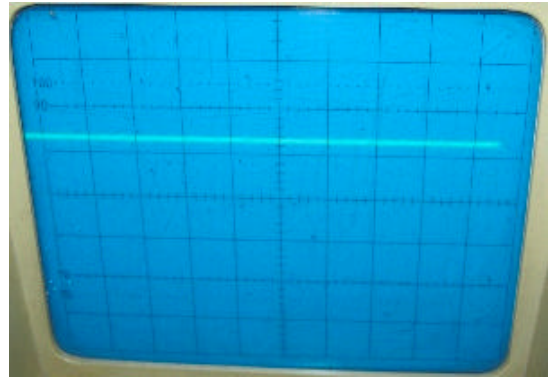


Fig. 27: Oscillogram of load voltage

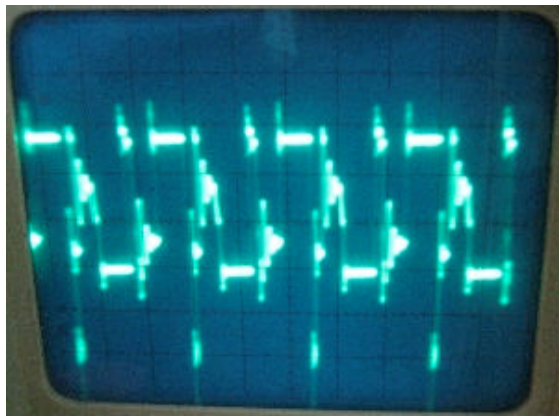


Fig. 25: Voltage across the primary X axis 1 div = 0.02 m sec, Y axis 1 div = 30 V

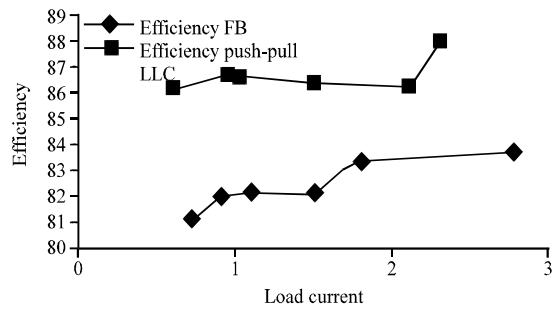


Fig. 28: Load current versus efficiency from experiment

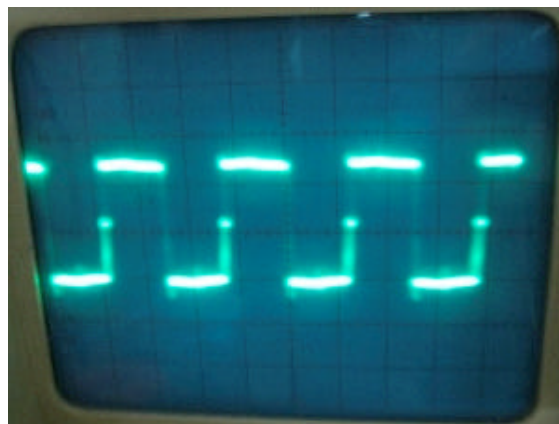


Fig. 26: Voltage across secondary X axis 1 div = 0.02 m sec, Y axis 1 div = 10 V

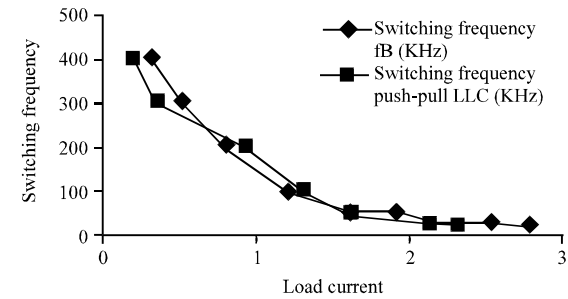


Fig. 29: Load current versus switching frequency from experiment

$R = 25\Omega$ ,  $C_7 = 100\mu$ ,  $L_1 = 28$  mH,  $L_p = 0.02$  mH and the switching frequency is 20 kHz. Experimental waveform of voltage across the primary is shown in Fig. 22 voltage across the secondary is shown in Fig. 23 and Oscillogram of load voltage is shown in Fig. 24.

**EXPERIMENTAL VERIFICATION OF PUSH-PULL LLC SERIES RESONANT CONVERTER**

The DC to DC converter was built and tested for push-pull LLC series resonant converter at 48V DC. The circuit parameters are as follows.

$R = 22\Omega$   $C_0 = 1000 \mu\text{F}$   $L_{\sigma} = 6 \text{ mH}$   $C_r = 2 \mu\text{F}$  and the switching frequency is 20 kHz. Experimental waveform of voltage across the primary is shown in Fig. 25 voltage across the secondary is shown in Fig. 26 and Oscillogram of load voltage is shown in Fig. 27.

### COMPARISON

From Fig. 9 and 24, output voltage of FB ZVS converter is nearly same as 12 V from simulation and experiment. From Fig. 17, efficiency of push-pull LLC converter is better than FB ZVS converter. From Fig. 20 and 21, switching stress of push-pull LLC converter is less than FB ZVS converter. From Fig. 16 and 27, output voltage of push-pull LLC is nearly same as 12V from simulation and experiment. From Fig. 18 and 28, load current versus efficiency of both converters are nearly same from simulation and experiment. From Fig. 19 and 29, load current versus switching frequency of both converters are nearly same from simulation and experiment. From Fig. 28, the efficiency of the FB ZVS converter is less than push-pull LLC converter and decreases at light load but keep the efficiency curve flat over a wide load current range. From Fig. 28 and 29, the switching frequency operating range varies from 20 to 300 kHz which matches to the simulation results diagram of Fig. 18 and 19, to some extent and keep the frequency curve flat over a wide load range for both converters. At low power and high efficiency requirement push-pull LLC series resonant converter is better than FB ZVS converter.

### CONCLUSIONS

Soft switched ZVS DC to DC converters are analysed, simulated, tested and results are presented using full bridge and push-pull LLC series resonant converter. Conversion of 48V to 12V is done using two methods and results are compared. At low power applications like battery charging high efficiency and low switching stress must be maintained from no load to full load. It appears that push-pull LLC series resonant converter is better than modified FB converter. The experimental results coincide with the simulation results.

### REFERENCES

Ayyanar, R. and N. Mohan, 2001. Novel soft-switching DC-DC converter with full ZVS-range and reduced filter requirement. I. Regulated-output applications. *IEEE Trans. Power Electron.*, 16: 184-192.

Boonyaroonate, I. and S. Mori, 2002. A new ZVCS resonant push-pull DC/DC converter topology. *IEEE APEC.*, 2: 1097-1100.

Borage, M., S. Tiwari, S. Bhardwaj and S. Kotaiah, 2008. A full-bridge DC-DC converter with zero-voltage-switching over the entire conversion range. *IEEE Trans. Power Electron.*, 23: 1743-1750.

Chen, W., F.C. Lee, M.M. Jovanovic and J.A. Sabate, 1995. A comparative study of a class of full bridge zero-voltage-switched PWM converters. *Proc. IEEE APEC.*, 2: 893-899.

Chen, W., Z. Lu, X. Zhang and S. Ye, 2008. A novel ZVS step-up push-pull type isolated LLC series resonant DC-DC converter for UPS systems and its topology variations. *Proceedings of the 23rd Annual IEEE Applied Power Electronics Conference and Exposition*, Feb. 24-28, Austin, pp: 1073-1078.

Jain, P.K., W. Kang, H. Soin and Y. Xi, 2002. Analysis and design considerations of a load and line independent zero voltage switching full bridge DC/DC converter topology. *IEEE Trans. Power Electron.*, 17: 649-657.

Jang, Y. and M.M. Jovanovic, 2004. A new family of full-bridge ZVS converters. *IEEE Trans. Power Electron.*, 19: 701-708.

Lee, B.Y., F.C. Zhang, A.J.G. Huang, 2002. LLC resonant converter for front end DC/DC conversion. *Applied Power Electron. Conf. Exposit.*, 2: 1108-1112.

Liu, T., Z. Zhou, A. Xiong, J. Zeng and J. Ying, 2006. A novel precise design method for LLC series resonant converter. *Proceedings of the 28th Annual International Telecommunications Energy Conference*, Sept. 2006, Providence, pp: 1-6.

Mason, J. and P.K. Jain, 2005. New phase shift modulated ZVS full-bridge DC/DC converter with minimized auxiliary current for medium power fuel cell application. *Proceedings of the IEEE 36th Power Electronics Specialists Conference*, June 16-16, Recife, pp: 244-249.

Padmanabhan, S., Y. Sukhi and Y. Jeyashree, 2007. Analysis design and development of regulated power supply-using soft switched resonant converters. *J. Applied Sci.*, 7: 3530-3535.

Pavlovsky, M., S. de Haan and J.A. Ferreira, 2009. Reaching high power density in multikilowatt DC-DC converters with galvanic isolation. *IEEE Trans. Power Electron.*, 24: 603-612.

Redl, R., N.O. Sokal and L. Balogh, 1991. A novel soft-switching full-bridge DC/DC converter: Analysis, design considerations and experimental results at 1.5 kW, 100 kHz. *IEEE Trans. Power Electron.*, 6: 408-418.

- Ryan, M.J., W.E. Brumsickle, D.M. Divan and R.D. Lorenz, 1998. A new ZVS LCL-resonant push-pull DC-DC converter topology. *IEEE Trans. Ind. Appl.*, 34: 1164-1174.
- Sabate, J.A., V. Vlatkovic, R.B. Ridley and F.C. Lee, 1991. High-voltage, high-power, ZVS, full-bridge PWM converter employing an active snubber. *Proceedings of the 6th Annual Applied Power Electronics Conference and Exposition*, Mar. 10-15, Dallas, TX, USA., pp: 158-163.
- Wei, C., G. Yilei and L. Zhengyu, 2007. A novel three level full bridge resonant Dc-Dc converter suitable for high power wide range input applications. *Proceedings of the 22nd Annual IEEE Applied Power Electronics Conference*, Feb. 25-Mar. 1, Anaheim, CA, USA., pp: 373-379.